Core-Collapse Supernova Explosions

Magneto-Rotational Mechanism

Luc Dessart

(University of Arizona; Princeton University)

Adam Burrows, Christian Ott, Eli Livne, Jeremiah Murphy, Ivan Hubeny

Mechanisms of Explosion

Neutrino: $L_\nu \sim 10\,\mathrm{B\,s^{-1}}$; $E_{\mathrm{dep}} \sim 0.1 \int_0^{\mathrm{few100ms}} L_\nu dt$

Acoustic: $L_{\mathrm{sound}} \sim 1\,\mathrm{B\,s^{-1}}$; $E_{\mathrm{dep}} \sim 1 \int_0^{\mathrm{1s}} L_{\mathrm{sound}} dt$

Magneto-rotational: E_{rot} tapped through magnetic stresses:

$$E_{\mathrm{rot}} \propto 1/r^2 \mathrm{during\,collapse};\, E_{\mathrm{rot}} \propto \Omega^2$$

E_{rot} ~ 10B for a ~2ms-period neutron star!

Do Fast-Rotating Fe or O/Ne/Mg cores exist?

B-fields: Torques tend to establish solid-body rotation and spin down the core during the pre-SN evolution (Spruit)

Mass Loss: Radiation driven winds + rotation:
Metallicity (Z) dependence & Rotation Dependence =>
Polar enhanced mass loss with little angular momentum loss
BUT Centrifugally-driven mass loss

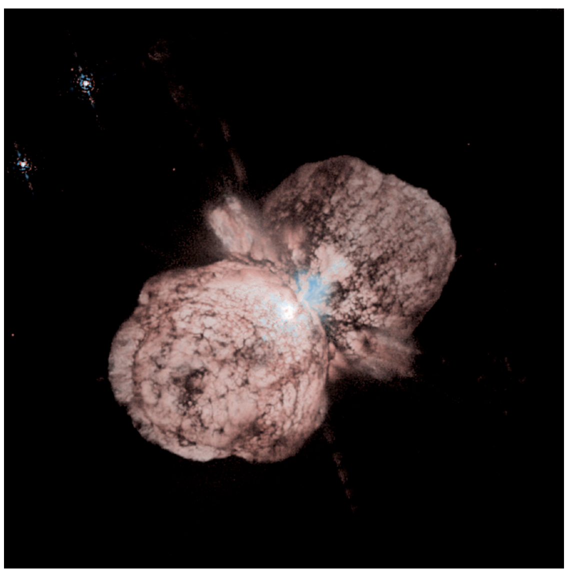

$$\dot{M} \propto Z^{0.5-0.8}$$

$$\dot{m} = \dot{M}/4\pi R^2$$

$$\dot{m} \propto F^{1/\alpha} g_{\rm eff}^{1-1/\alpha}$$

$$g_{\rm eff} = \frac{GM}{R^2}(1 - \kappa_e F/gc - \Omega^2 \sin^2\theta)$$

$$\frac{\dot{m}(\theta)}{\dot{m}(0)} = 1 - \Omega^2 \sin^2\theta$$

Stellar Evolution Models

Example of ``collapsar-candidate'' models of WH06 (35OC), Yoon & Langer (2005; A40f0.4h) and C. Georgy (2007)

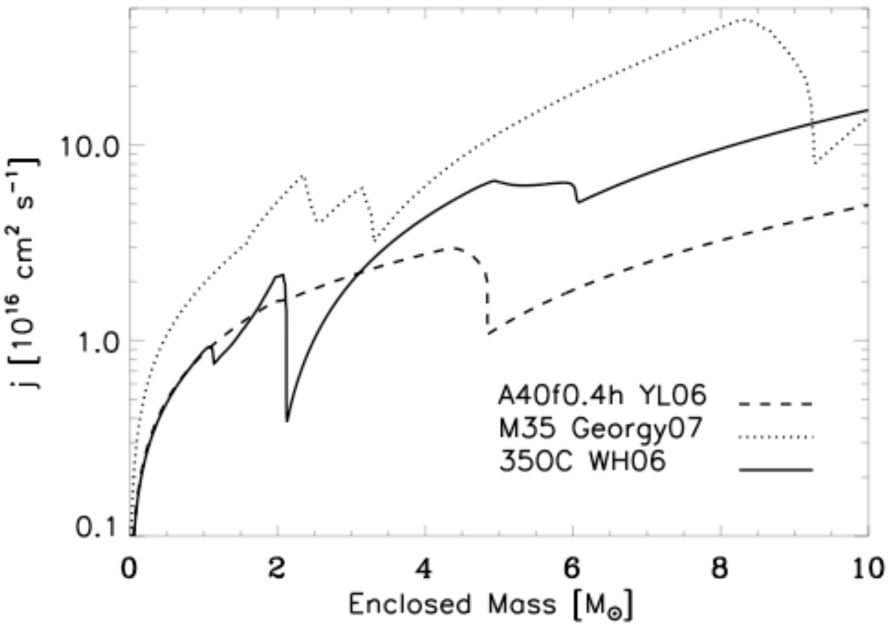

High M and Ω => $\tau_{mixing} < \tau_{nuc}$ => Chemically-homogeneous evolution => no RSG phase and no large torques

Stellar evolution models suggest **fast-rotators** are to be found in **low-metallicity** environments or may require **binary-evolution** channell

(see Woosley/Heger, Yoon/Langer, Maeder/Meynet)

Magnetically-field Amplification

- Flux freezing during collapse: $B/B_0 \propto (\rho_{\rm nuclear}/\rho_0)^{2/3} \sim 1000$
- Winding of the poloidal field

$$\frac{\partial B_\phi}{\partial t} \sim B_P \left(\frac{\partial \Omega}{\partial \ln r}\right) \qquad \Delta B_\phi \sim B_P \Omega t \sim B_P \left(\frac{2\pi t}{P}\right)$$

- Magneto-rotational Instability (MRI; requires differential rotation)

$$\tau_{mri} \sim 4\pi \left(\frac{\partial \ln r}{\partial \Omega}\right) \sim 2P \;\; ; \; \lambda_{mri}^{max} \sim \frac{2\pi v_A}{\Omega} \sim v_A P \sim 10^4 \text{ cm } P_{10} \frac{B_{12}}{\rho_{11}^{1/2}}$$

- Fields at saturation estimated from equipartition with E_{rot}

$$B \sim \sqrt{4\pi\varepsilon\rho r^2 \Omega^2} \sim 10^{15} \text{ G} \sqrt{\frac{\varepsilon}{0.1}} \sqrt{\rho_{11} r_{30}^2} \left(\frac{\Omega}{10^3 \text{ rad s}^{-1}}\right)$$

Characteristic MRI time and spatial scales

(model taken from Burrows et al. 2007)

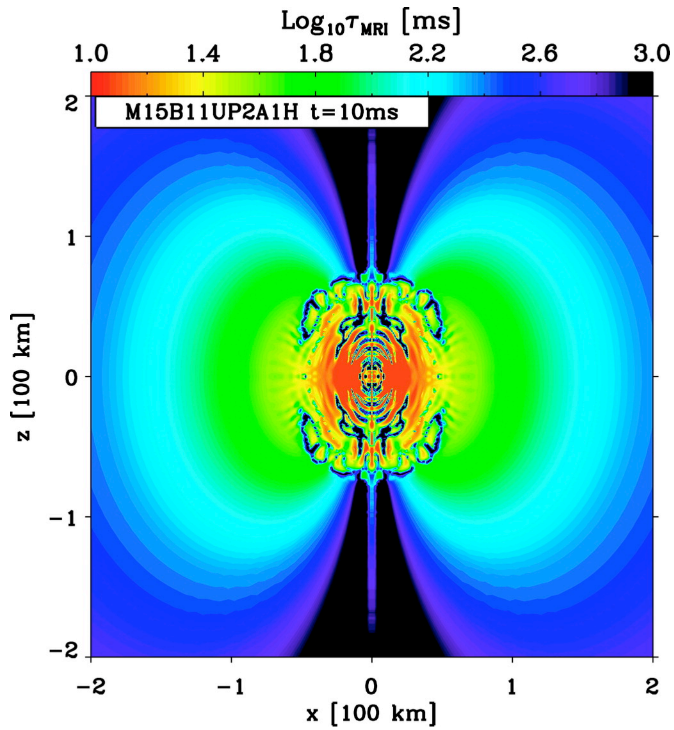

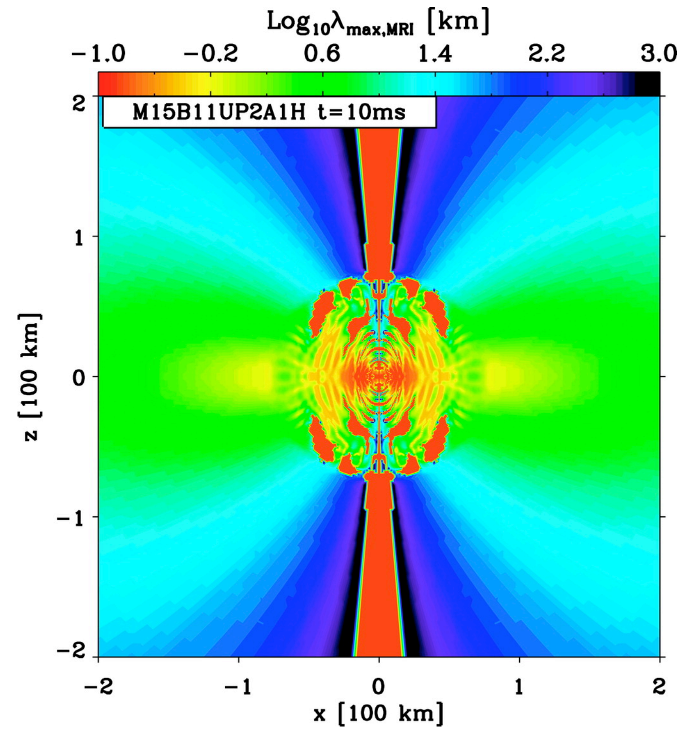

Even for such large post-bounce fields, our resolution of <1km is still insufficient

Ansatz: Set initial fields so that by compression and winding alone, we obtain fields at saturation that are comparable to what would obtain were we to resolve the MRI

Magnetically-driven Core-Collapse SN Explosions

Burrows et al. (2007); Dessart et al. (2007)

TABLE 1

Properties of Models

Name	Mass ($M_{\odot}$)	$B_{poloidal}$ (G)	Field Geometry	P_0 (s)	A_0 (km)	$\Delta\theta$ (deg)	$t_{explosion}$ (ms)	t_{end} (ms)	v_{max} (km s^{-1})	$E_{explosion}$ (10^{51} ergs)	Power (10^{51} ergs s^{-1})	$\langle P \rangle$ (ms)
M15B0DP2A1H	15	0	...	2	1000	90	...	595	...	...	...	3.70
M15B10DP2A1H	15	10^{10}	Dipole	2	1000	90	550	944	37000	0.03	0.155	3.14
M15B10DP2A1F	15	10^{10}	Dipole	2	1000	180	550	685	37000	0.03	0.118	3.18
M15B11DP2A1H	15	10^{11}	Dipole	2	1000	90	250	636	50000	0.2	0.661	6.17
M15B11UP2A1H	15	10^{11}	Uniform	2	1000	90	180	585	55000	2.0	6.832	3.98
M15B11DP4A1H	15	10^{11}	Dipole	4	1000	90	170	415	33000	0.005	0.050	4.21
M15B12DP2A1H	15	10^{12}	Dipole	2	1000	90	80	111	36000	0.6	3.168	25.60

- MHD multi-group flux-limited-diffusion VULCAN/2D simulations
- Input structure: Model m15b6 (Heger et al. 2005)
- Shen EOS
- Neutrino opacities & emissivities (Burrows et al. 2006)
- Field configuration: Dipolar or uniform ($B=B_z$), strength from 10^{10} to 10^{12}G (initially, $B_p >> B_\phi$)
- Rotation: Ω-cst inside to j-cst outside
- Coverage: 90^o or 180^o.

Results from Magnetically-driven Explosions

Burrows et al. (2007)

$P_{mag} << P_{gas}$ inside PNS, but $P_{mag} \sim P_{gas}$ outside of PNS at late times

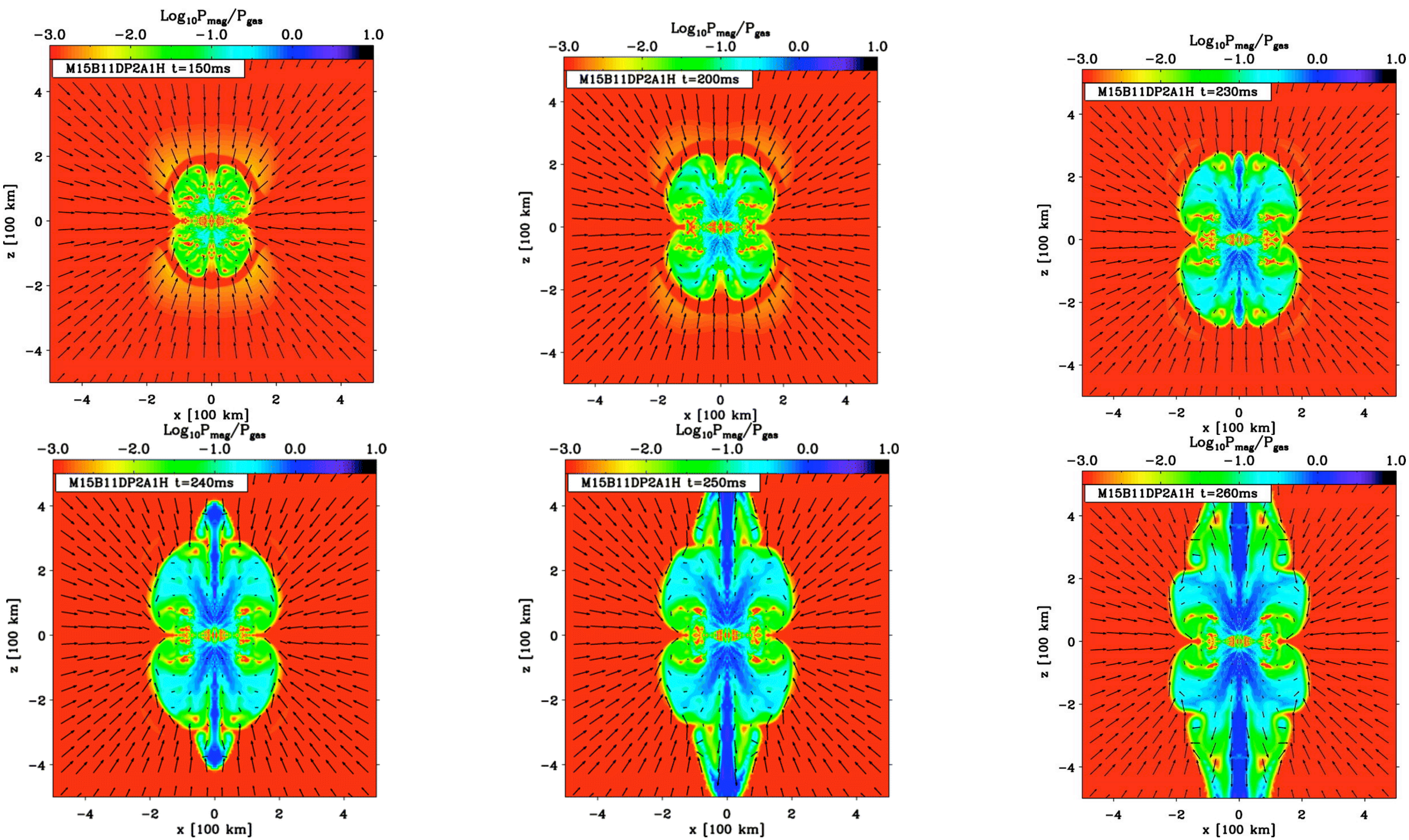

Results from Magnetically-driven Explosions

Burrows et al. (2007)

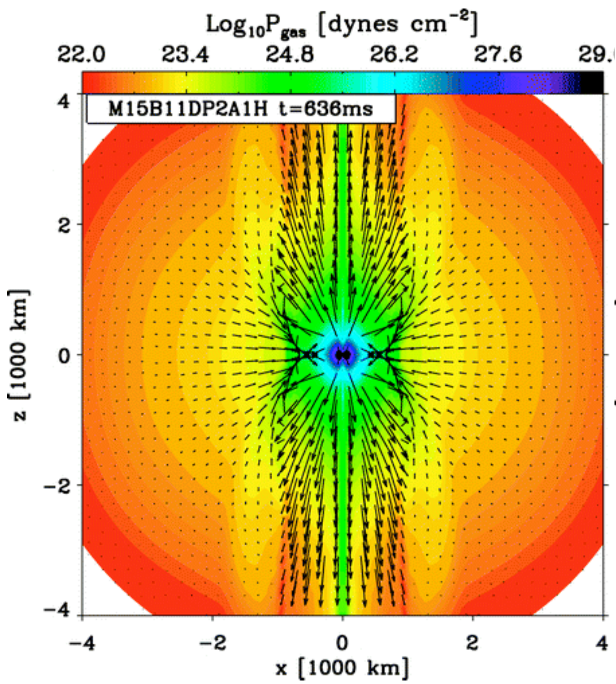

(Bernoulli vector)

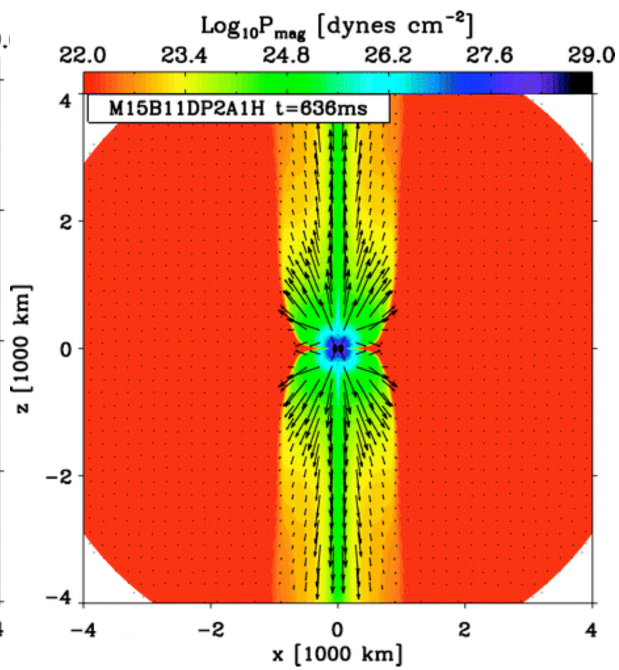

$\vec{S} = c/4\pi(\vec{E} \times \vec{B})$ vector

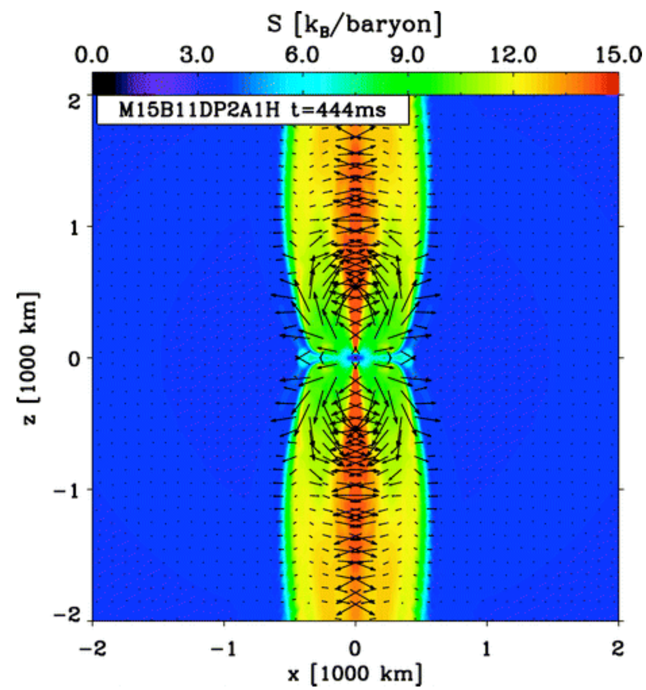

$(\nabla \times \vec{B}) \times \vec{B}$ vector

Fluid energy flow

Electromagnetic-energy flow

Magnetic-confinement

Results from Magnetically-driven Explosions

Burrows et al. (2007)

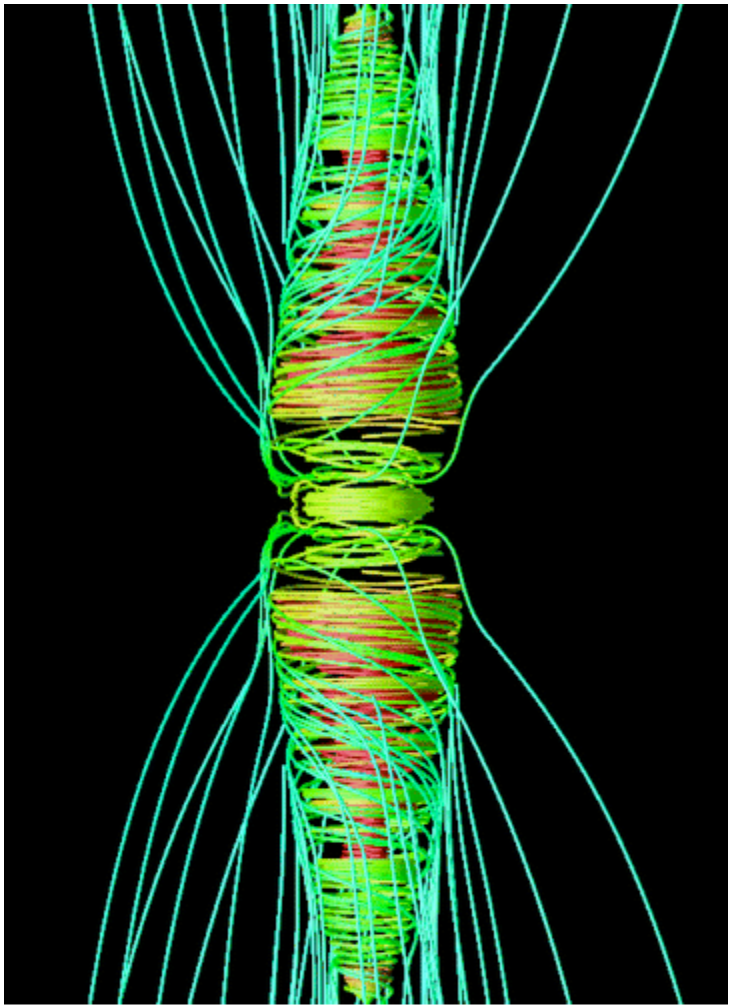

M15B11DP2A1H - t = 265 ms

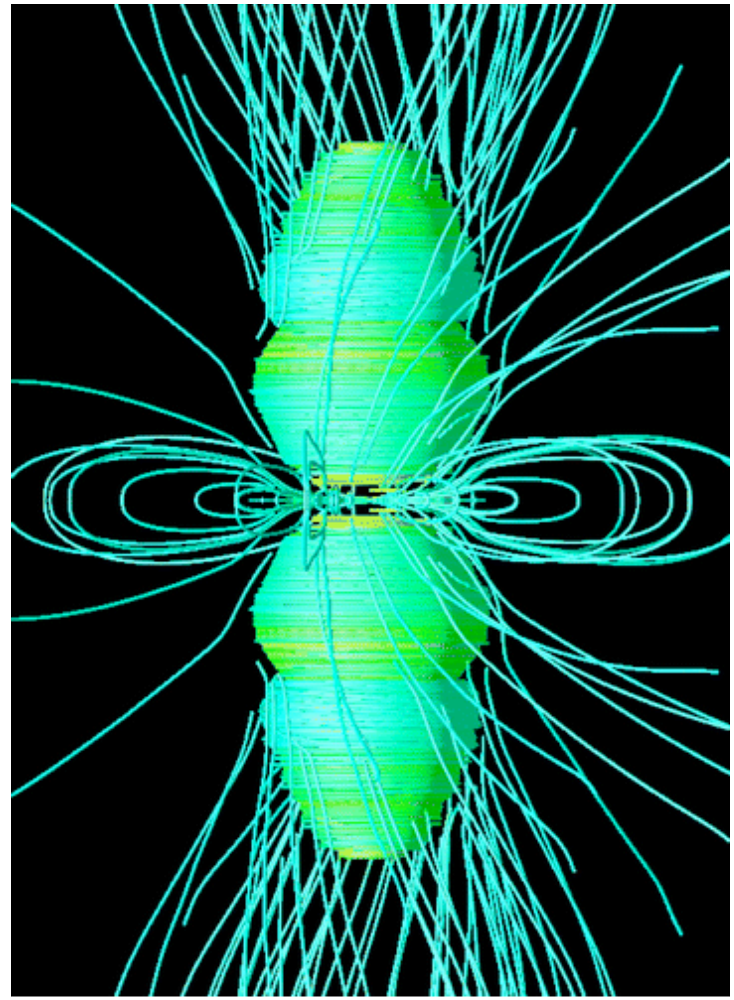

M15B10DP2A1H - t = 885 ms

Magnetically-driven Core-Collapse SN Explosions

Burrows et al. (2007)

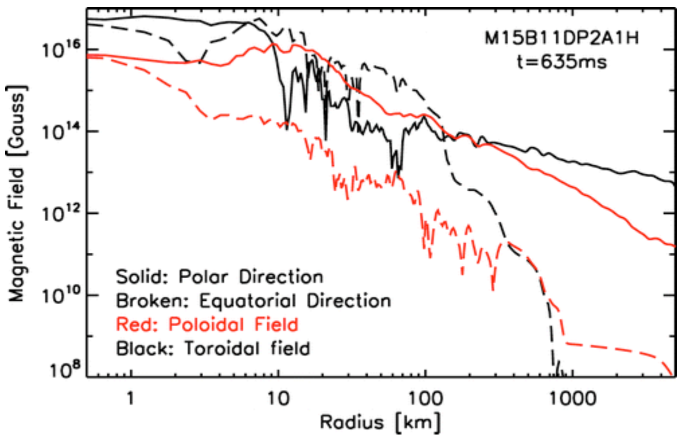

- Magnetar-like field strengths inside PNS
- $B_{tor} > B_{pol}$ (winding; no MRI)
- B_{pol} increased by advection/stretching of toroidal field lines

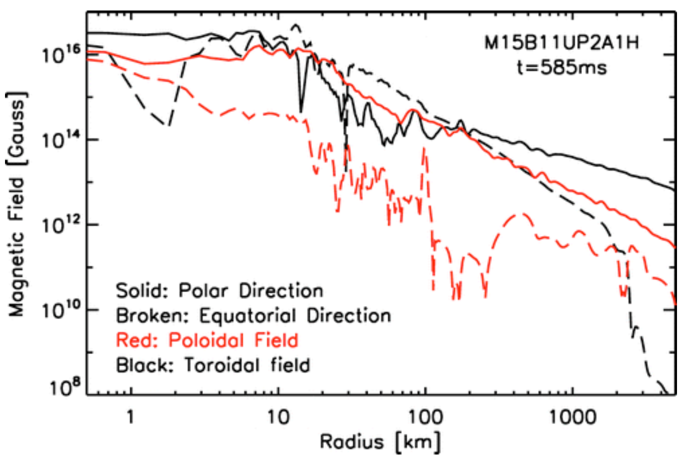

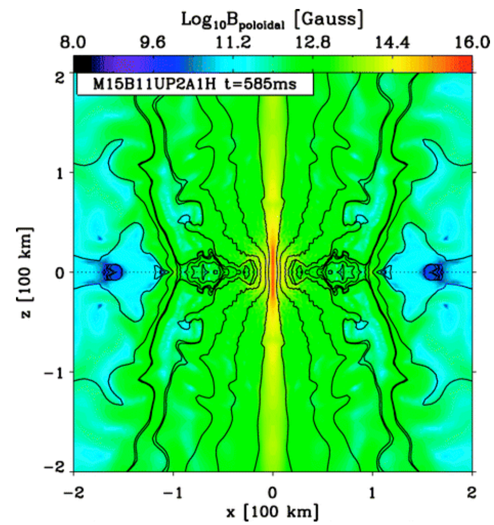

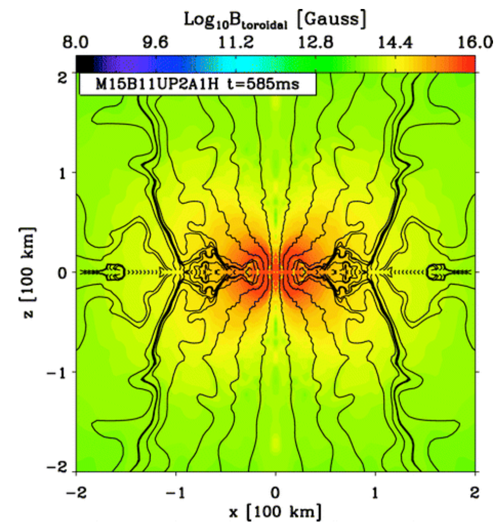

Magnetically-driven Core-Collapse SN Explosions

Burrows et al. (2007)

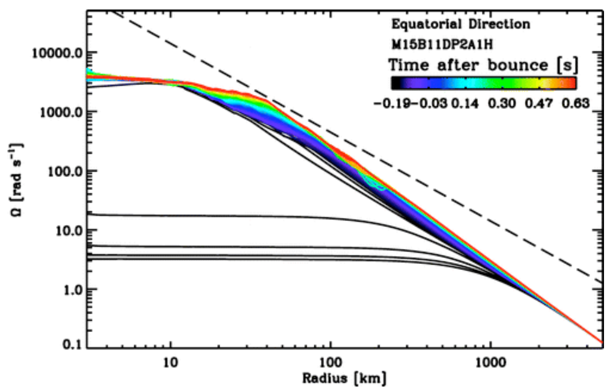

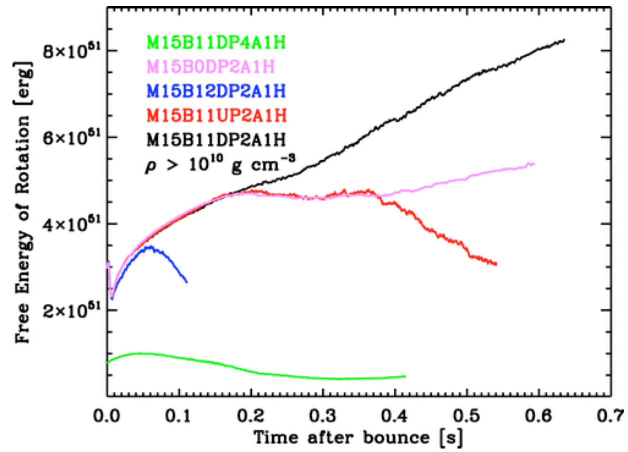

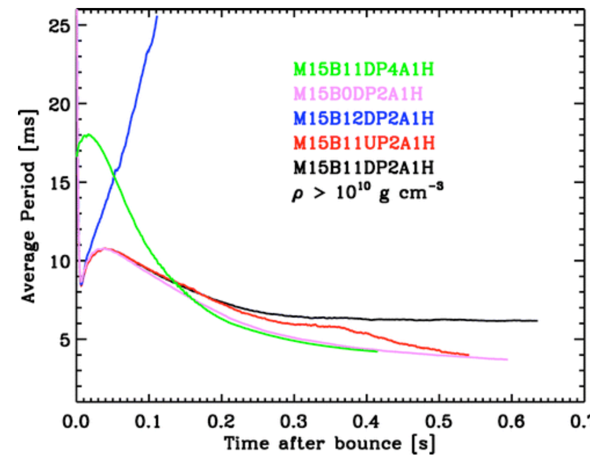

- Solid body rotation inside
- Differential Rotation outside => suitable for growth of MRI
- Large reservoir of free rotation energy
- PNS spin-down

Magnetically-driven Core-Collapse SN Explosions

Burrows et al. (2007)

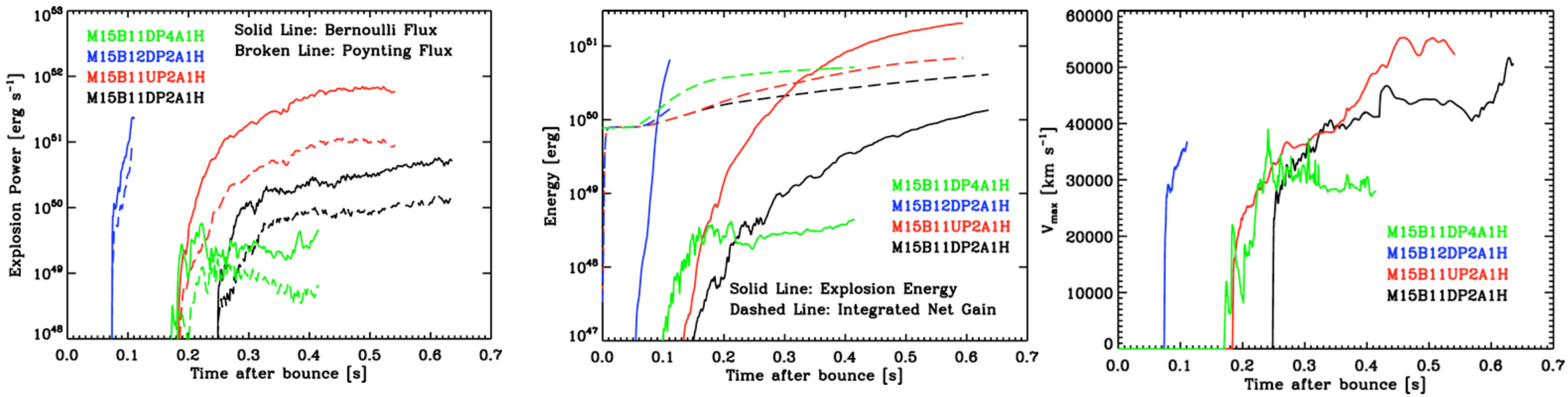

- Sub-dominant contribution from neutrinos compared to Bernouilli and Poynting powers
- Hypernova like explosion energies
- Baryon-loaded non-relativistic ejecta

Results from Magnetically-driven Explosions

Burrows et al. (2007)

- $P_{mag} \sim P_{gas}$ at 30-100km and ~200ms after bounce
- **Baryon-loaded Non-relativistic Jet-like Explosions**
- Hypernova (~10B) explosion energies
- Rotation is key; Neutrino contribution is secondary
- Extraction of core rotation by magnetic stresses
- Neutron-star spin-down

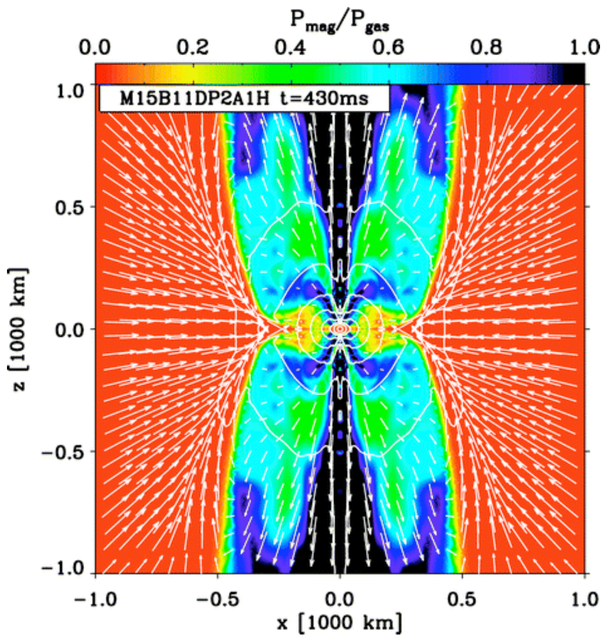

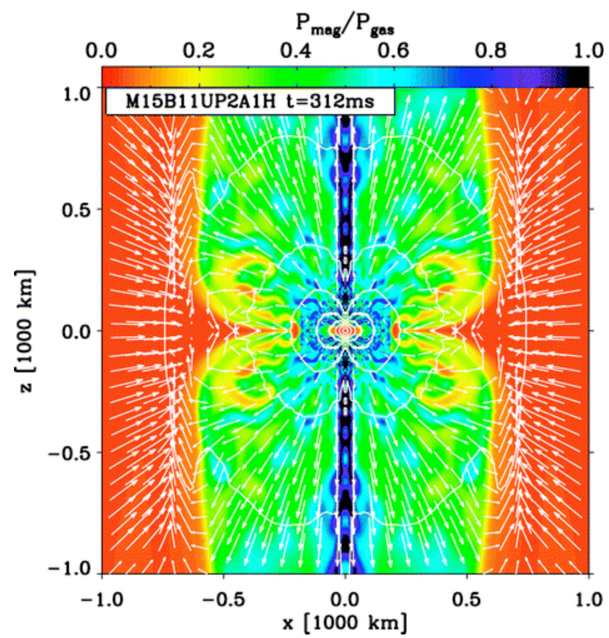

The Collapsar model

Woosley (1993), MacFadyen & Woosley (1999)

Key Role Played by Rotation

- **Failed SN** forming a 2-3M_{sun} **BH** from a **WR-star** progenitor.
- **Outcomes** function of j_{16}=j/10^{16} cm^2s^{-1}
- j_{16} **< 3** : Material falls into the BH uninhibited
- j_{16} **> 20** : Material infall halted by centrifugal acceleration
- **3<j_{16}<20**: **quasi-Keplerian disk** forms above the BH.

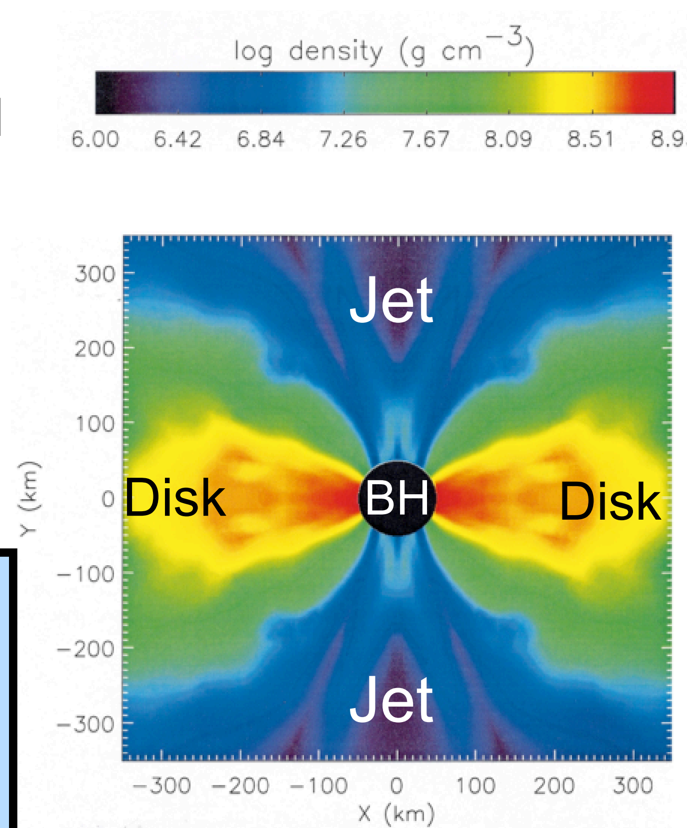

Relativistic Jet (and GRB) **+**	*SN Explosion*
(~1 B)	(~10 B)
(Baryon-free)	*(Baryon-loaded)*
(Along the Poles)	*(From the Disk)*

The Proto-neutron Star Phase of the Collapsar Model and the Route to Long-soft Gamma-ray Bursts and Hypernovae

Dessart et al. (2008)

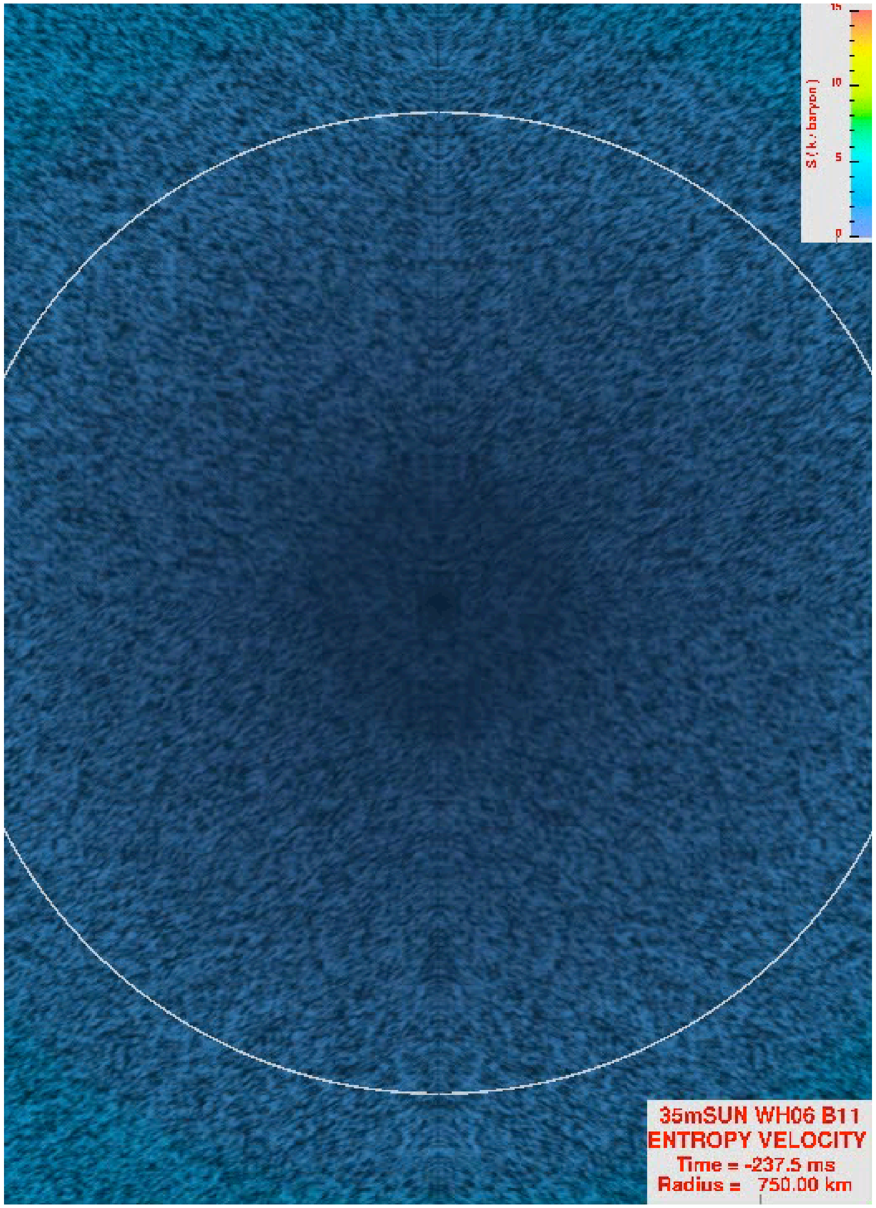

Simulation of the 35-M_{sun} collapsar-candidate model of Woosley & Heger (2006) using their initial ρ, T, Ω, $B_{toroidal}$, and $B_{poloidal}$ distributions, but enhancing $B_{poloidal}$ by a factor of 5 to mimick the MRI field amplification

Progenitor: fast-rotating massive main-sequence star evolved **chemically homogeneously** at low metallicity.

dM/dt Explosion > dM/dt Accretion

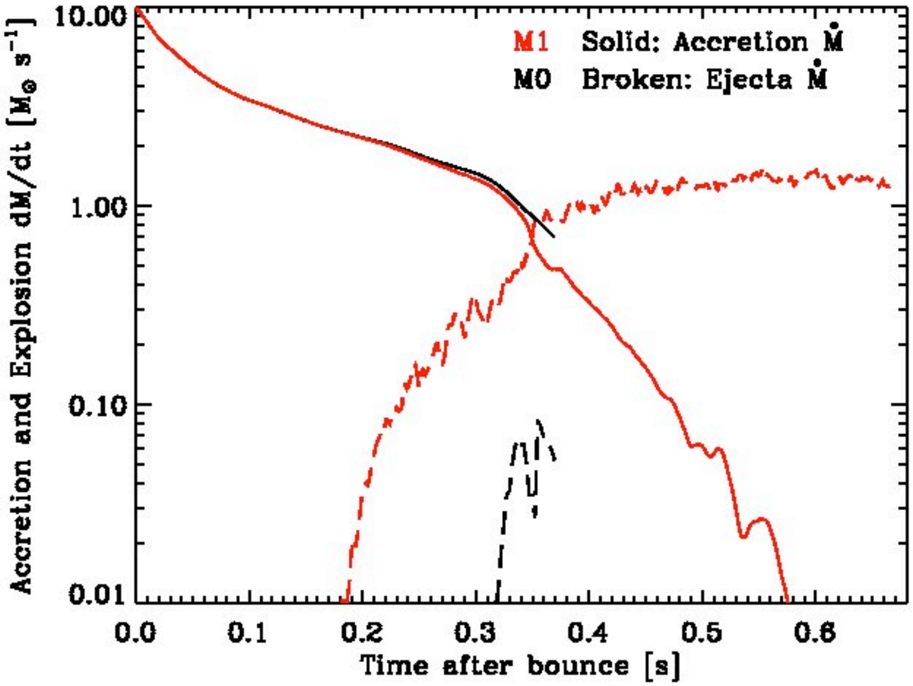

M_{PNS} Decreases with Time

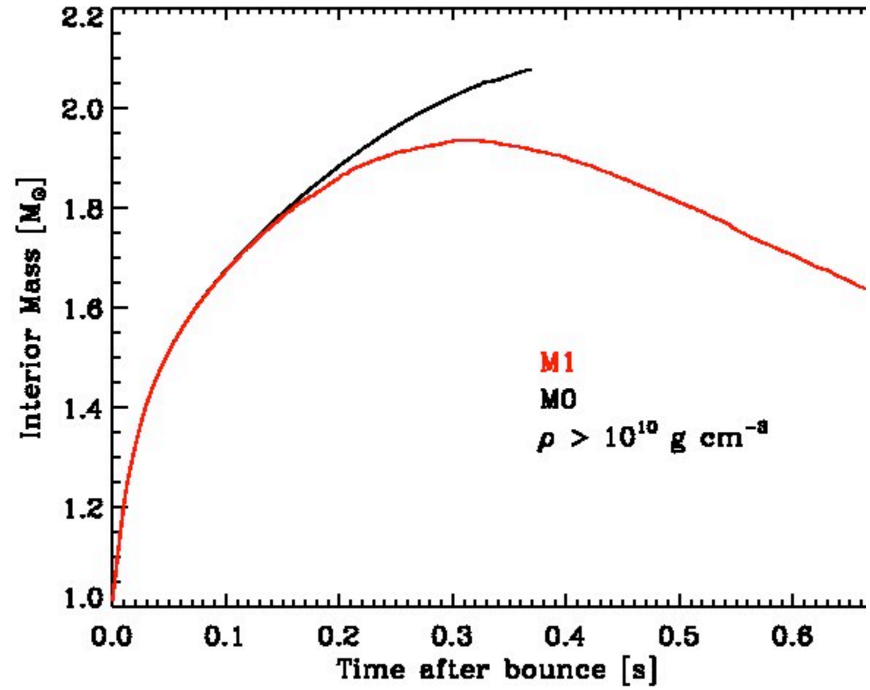

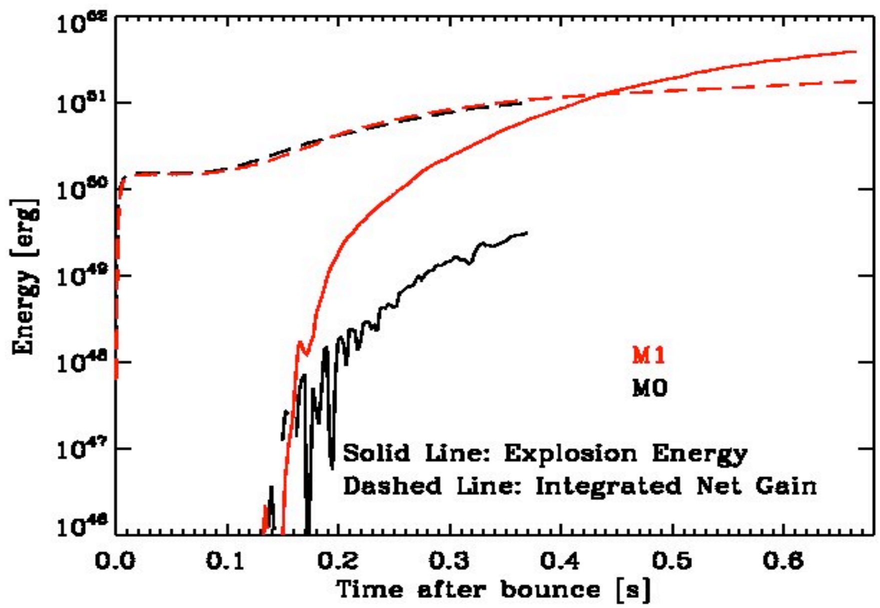

Hypernova Energy: ~3B at 700ms

Conclusions

I. Provided the MRI operates at the surface of the ms-period NS, a magnetically-driven explosion ensues during the PNS phase, in the form of a baryon-loaded non-relativistic jet, and a **BH, central to the collapsar model, does not form**.

II. Current models of chemically homogeneous evolution at low metallicity yield massive stars with iron cores that may have ***too much*** angular momentum to avoid a magnetically-driven explosion in the immediate post-bounce phase.

III. Fast rotation in the iron core may inhibit collapsar formation, which requires a large angular momentum **not in the core but *above* it.**

IV. Variations in the angular momentum distribution of massive stars at core collapse might explain both the diversity of Type Ic SNe/HNe and their possible association with a GRB.

V. Rather than the progenitor mass, the **angular momentum distribution**, through its effect on magnetic field amplification, distinguishes these outcomes.